# Optical and Polarity Control of Donor–Acceptor Conformation and Their Charge Transfer States in Thermally Activated Delayed Fluorescence Molecules

*Paloma L. dos Santos,[a] Jonathan S. Ward,[b] Andrei S. Batsanov,[b] Martin R. Bryce,[b] Andrew P. Monkman[a*]*

a. OEM Research Group, Physics Department, Durham University, South Road, Durham DH1 3LE, UK

b. Department of Chemistry, Durham University, South Road, Durham DH1 3LE, UK

**ABSTRACT**

This study reports two novel D–A–D molecules, 2,7-bis(phenothiazin-10-yl)-9,9-dimethylthioxanthene-*S,S*-dioxide (DPT-TXO2) and 2,7-bis(1-methylphenothiazin-10-yl)-9,9-dimethylthioxanthene-*S,S*-dioxide (DMePT-TXO2), where the latter differs by only a methyl group incorporated on each of the donor units. DMePT-TXO2 in solution and solid state shows dual charge transfer (CT) emission. The CT states come from two distinctive conformations between the D and A units. Experiments show that the emission contribution of each state can be controlled by the polarity of the environment and by the excitation energy. Also, how the different conformers can be used to control the TADF mechanism is analyzed in detail. These results are important as they give a more in-depth understanding about the relation between molecular conformation and the TADF mechanism, thereby facilitating the design of new TADF molecules.

## INTRODUCTION

Organic light-emitting diodes (OLEDs)[1] are established in display and lighting applications, but, understanding how to design new molecules which show strong thermally activated delayed fluorescence (TADF) is crucial in order to achieve highly efficient OLEDs. The TADF mechanism uses thermal energy to vibrationally couple local triplet and triplet CT states (dark states) such that the triplet energy can cross back to emissive CT singlet states by reverse intersystem crossing (rISC), thereby overcoming the 25% internal quantum efficiency limit imposed by spin statistics.[2–6]

In order to maximize TADF, the energy splitting between the singlet and triplet states ($\Delta E_{ST}$) should be minimized. A common strategy involves designing organic molecules with nearly orthogonal D–A units that show intramolecular excited states with strong charge transfer character (CT). We recently identified that the spin orbit coupling (SOC) mechanism in TADF systems is a complex second-order process requiring vibronic coupling between $^3$CT (charge transfer state) and $^3$LE (local state) to mediate the spin flip back to the $^1$CT state.[7,8] Thus, $^3$CT and $^3$LE are equally important in the analysis of the $\Delta E_{ST.}$

However, the near orthogonality of D and A units does not guarantee the existence of strong CT characteristics and an efficient TADF mechanism. Ward and co-workers[9] showed that increasing steric restriction around the D–A bond changes the photophysics and effects the TADF mechanism in rigid nearly orthogonal D–A–D molecules. However, further work is still necessary to fully understand how the efficiency of the TADF mechanism is affected by this steric restriction.

In this work, CT states, which show complex photophysics because they are sensitive to the environment and molecular conformation, are studied in detail for two novel D–A–D type

molecules, 2,7-bis(phenothiazin-10-yl)-9,9-dimethylthioxanthene-*S*,*S*-dioxide (DPT-TXO2) and 2,7-bis(1-methylphenothiazin-10-yl)-9,9-dimethylthioxanthene-*S*,*S*-dioxide (DMePT-TXO2). These two molecules differ only by a methyl group incorporated on each of the donor units, however, dramatic differences in the photophysical properties are observed. Particularly, we show that different molecular conformations give rise to different CT states, termed axial ($CT_{ax}$) and equatorial ($CT_{eq}$). Recent works have also observed this dual fluorescence from CT states in different organic molecules, and they have assigned the different conformers as a result of the folding of the phenothiazine donor units.[10–12] Here, we show how the different conformers can be controlled by the polarity of the environment and by the excitation energy. Moreover, we discuss how the different conformers can be used to control the TADF mechanism.

## EXPERIMENTAL SECTION

The synthesis and structural characterization of 2,7-bis(phenothiazin-10-yl)-9,9-dimethylthioxanthene-*S*,*S*-dioxide (DPT-TXO2) and 2,7-bis(1-methylphenothiazine-10-yl)-9,9-dimethylthioxanthene-*S*,*S*-dioxide (DMePT-TXO2) are given in detail in the supplementary information (**S1**). Two types of samples were studied in this work: solutions ($10^{-3}$ to $10^{-5}$ M) and films produced in zeonex matrix (organic material 2.5 mg/mL:zeonex 180 mg/mL 1:1 *v/v*). All the solutions were diluted in different solvents and stirred for several hours. They also were degassed to remove all the oxygen dissolved in the solutions by four freeze-pump-thaw cycles to perform the degas test and delayed fluorescence measurements. The films in zeonex matrix were fabricated by drop casting onto quartz substrates.

Steady state absorption and emission spectra were acquired using a UV-3600 Shimadzu spectrophotometer and a Jobin Yvon Horiba Fluoromax 3, respectively. Time resolved spectra

were obtained by exciting the sample with a Nd:YAG laser (EKSPLA), 10 Hz, 355 nm/266 nm or by using a Nitrogen laser, 10 Hz, 337 nm. Sample emission was directed onto a spectrograph and gated iCCD camera (Stanford Computer Optics). Photoluminescence quantum yelds (PLQY) were acquired using PLQY Quantaurus – QY Hamamatsu. The PLQY values (5% error) were calculated from the average of 4 values obtained with excitation between 270 and 300 nm (10 nm step), region where DPT-TXO2 and DMePT-TXO2 show strong absorption.

X-ray crystal structures were determined using a Bruker 3-circle D8 Venture diffractometer with a PHOTON 100 CMOS area detector, using Mo-$K_\alpha$ (DPT-TXO2) and Cu-$K_\alpha$ (DMePT-TXO2) radiation from IμS microsources with focussing mirrors. Crystals were cooled to 120 K using a Cryostream (Oxford Cryosystems) open-flow $N_2$ gas cryostat. The structures were solved by direct methods using SHELXS 2013/1 software,[13] and refined by full-matrix least squares using SHELXL 2014/7[14] and OLEX2[15] software. DPT-TXO2 crystallized from DCM/hexane solution as a DPT-TXO2·$CH_2Cl_2$ solvate. The structure of DMePT-TXO2 contains infinite solvent-accessible channels parallel to the *x* axis and amounting to *ca*. 20% of the crystal space (**Figure S2**). The channels are occupied by disordered solvent, tentatively estimated as one hexane and 1.5 $CH_2Cl_2$ molecules per unit cell, or half of this per formula unit. The solvent contribution to the structure factors was eliminated using PLATON SQUEEZE solvent-masking procedure[16] estimating the diffuse electron density in the voids as 112 *e* per unit cell. Full crystallographic data have been deposited with the Cambridge Structural Database, CCDC-1426132 (DPT-TXO2) and 1426133 (DMePT-TXO2).

## RESULTS AND DISCUSSION

### 1. X-RAY ANALYSES

**Figure 1** shows the X-ray molecular structure of DPT-TXO2 and DMePT-TXO2 in different viewing angles. DPT-TXO2 has no crystallographic symmetry but an approximate mirror plane through the S, O, C(7) and methyl carbon atoms. The TXO2 system (acceptor unit) is folded along the S(1)…C(7) vector, its arene rings *i* and *ii* forming a dihedral angle of 139.1º, cf. 137.8º in DPO-TXO2 and 133.9º in unsubstituted TXO2.[17] Both phenothiazine moieties are moderately folded along the N…S vectors, with inter-arene angles *iii/iv* 162.0º and *v/vi* 154.4º. The near-perpendicular twists around C(4)-N(1) and C(10)-N(2) bonds (86.0º and 80.1º, respectively) effectively preclude π-conjugation between donor and acceptor parts. These bonds are longer than N–C bonds within phenothiazine systems, average 1.438(1) vs 1.416(2) Å, indicating that the lone pairs of N interact predominantly with the phenothiazine arene rings. In DMePT-TXO2 the folding of the TXO2 unit is similar (dihedral angle *i/ii* 135.9º) but the phenothiazine conformation is entirely different. The 1-methylphenothiazine substituent at C(4) is disordered between two orientations with methyl groups on opposite sides, with nearly equal probability, 0.482(2) to 0.518(2). The substituent at C(10), however, is ordered. The latter is folded (dihedral angle *v/vi* 134.0º) stronger than the (un-methylated) phenothiazine in DPT-TXO2, but similarly to mono- or di-methylated phenothiazine in DBT derivatives (128.7-135.5º).[9] The twist around the C(10)-N(2) bond is negligible (0.9º) and this bond (1.408(3) Å) is considerably shorter than the other N(2)-C bonds (mean 1.434(3) Å). The geometry of the disordered phenothiazine is essentially similar (though less accurately determined), with the mean phenothiazine folding of *ca*. 135º and the twist around C(10)-N(2) bond of 16º (*A*) or 13º (*B*).

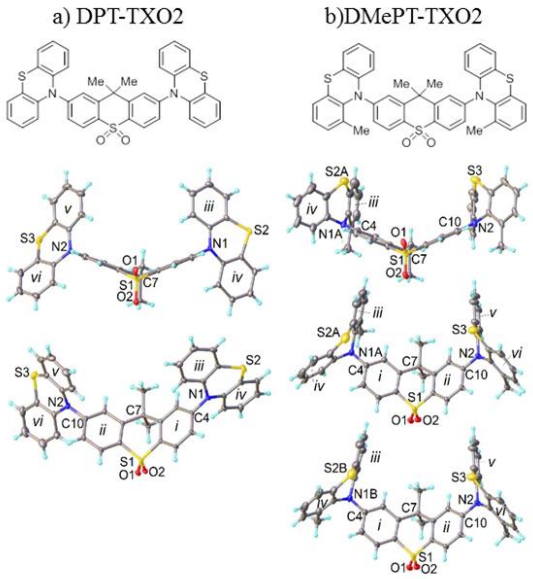


**Figure 1.** Chemical structures and X-ray molecular structures from different angles of a) DPT-TXO2 and b) DMePT-TXO2 (showing two conformers statistically mixed in the crystal). Thermal ellipsoids are drawn at the 50% (DPT-TXO2) and 30% (DMePT-TXO2) probability level.

Therefore, both molecules show a conformation with nearly perpendicular D–A orientation. The conformation shown by DPT-TXO2 is termed equatorial-equatorial (eq-eq) and DMePT-TXO2 axial-axial (ax-ax).[11,18] Given that in both conformations the D and A units are perpendicular, one could imagine strong CT character leading to strong TADF in both systems. However, dramatic differences in the photophysical properties of these molecules are observed, showing that the nearly perpendicular orientation is not sufficient to design TADF emitters.

## 2. SOLUTIONS PROPERTIES

**Figure 2a** shows the extinction coefficient spectra of DPT-TXO2 and DMePT-TXO2 and their individual D and A units, all in dichloromethane ($CH_2Cl_2$) solvent. DPT-TXO2 shows mainly the absorption band of the donor unit. DMePT-TXO2 shows a distinct absorption spectrum, at

higher energies compared to DPT-TXO2. **Figure S3** shows the absorption spectra of DPT-TXO2 and DMePT-TXO2 also in methylcyclohexane (MCH) and toluene. The absorption peak at lower energy shows a slight red shift by increasing the polarity of the solvent, which can be associated with $\pi \rightarrow \pi^*$ character of the transitions. By comparison to the individual D and A units, the extinction coefficients of the low energy bands in both D–A–D molecules is greatly enhanced. This increase in oscillator strength does not come from simple conjugation as the D–A units are orthogonal precluding such conjugation. Instead, this is a clear signature of state mixing, here the π-π* and n-π* states. The effect of state mixing has been described in detail by C. M. Marian[19] and T. J. Penfold;[20] of significance here is the effect of the methyl group on the donors of DMePT-TXO2. As these groups stabilise the H-extra (axial) conformation of the phenothiazine units[11] less of the bridging nitrogen lone pair couples into the donor increasing the π-π* character, and hence oscillator strength of the lowest energy transition, but at the expense of a blue shift. Whereas in DPT-TXO2, the H-intra conformation of the phenothiazine is stabilized and more of the bridging nitrogen lone pair couples into the donor increasing the *n*-π* character, decreasing the oscillator strength of the lowest energy transition and giving a more red shift.

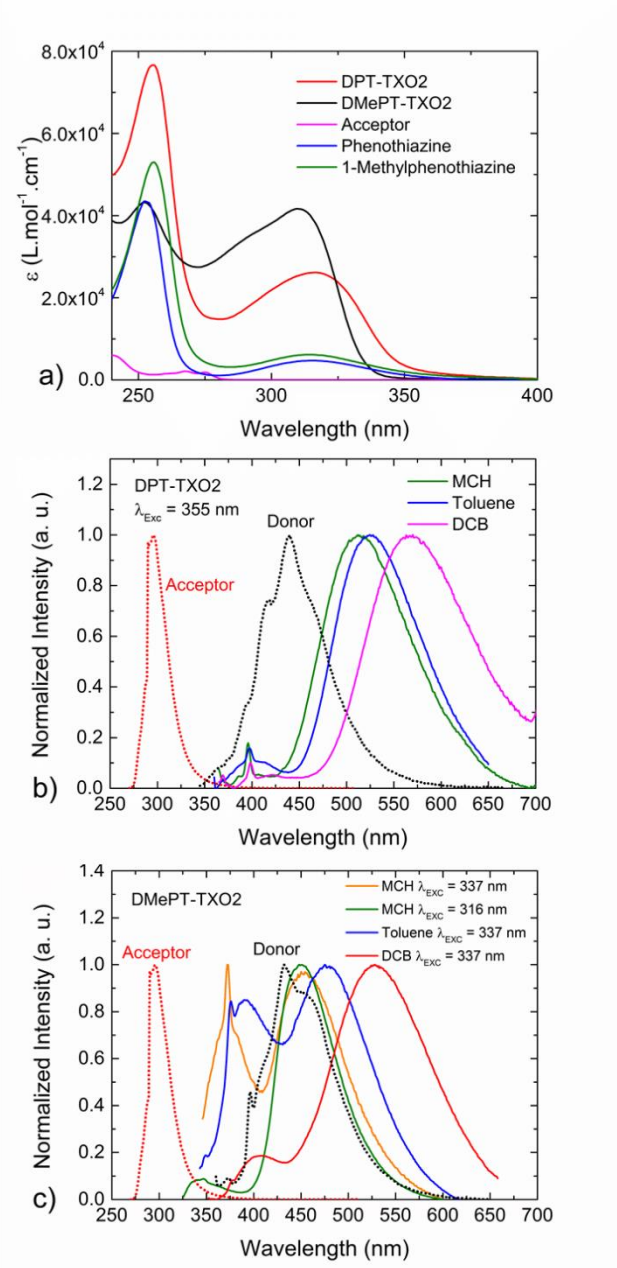


**Figure 2. a)** Extinction coefficient spectra of the DPT-TXO2, DMePT-TXO2 and their acceptor and donor units, all diluted in dichloromethane ($CH_2Cl_2$). b) Normalized photoluminescence (PL) spectra of acceptor, donor and DPT-TXO2 and c) DMePT-TXO2 molecules. Donor and acceptor units were diluted in methylcyclohexane (MCH) solvent and D–A–D in different solvents: MCH,

toluene and 1,2-dichlorobenzene (DCB). DPT-TXO2 molecules were excited at 355 nm and DMePT-TXO2 at 337/316 nm.

**Figure 2b** shows the emission spectra of DPT-TXO2 in different solvents. The spectra show clear and strong CT emission having a Gaussian band shape and strong red shift compared to the individual D and A emission spectra. The photoluminescence (PL) spectra move to longer wavelength with increasing the solvent polarity, showing a strong positive solvatochromism, as observed before in other D–A–D type molecules.[6,21–23] A vestige of emission from the donor unit or weak axial CT state, around 400 nm, is observed in all solvents. The $^1$CT emission does not depend on the excitation energy (See **Figure S4**).

The contribution of triplet excited states to the overall emission was determined by comparing the emission intensity in aerated and degassed solutions. The contributions of DF are 13%, 37% and 42% for MCH, toluene and DCB, respectively (**Figure S5**). The higher contribution of DF in DCB is due to the small CT-$^3$LE energy splitting ($\Delta E_{ST}$) achieved in this polar environment, thus, an efficient repopulation of $^1$CT state occurs *via* a reverse intersystem crossing (rISC) process from the $^3$LE state. The phosphorescence (PH) spectrum of DPT-TXO2 was identified in the solid state (**Figure 6d**), demonstrating that the PH onset is closest in energy to $^1$CT in DCB solvent, confirming that the shift in the energy of triplet levels is small with the change in the polarity of the environment.

DMePT-TXO2 shows much more complex emission spectra, with different emission bands in different polar environments and excitation energies. **Figure 2c** shows the emission spectra of all solutions (MCH, toluene and DCB) excited at 337 nm and also MCH solution excited at 316 nm. For the least polar solvent, MCH, the emission observed around 370 nm is associated with a weak CT state, coming from the axial-axial conformation ($CT_{ax\text{-}ax}$); which has strong local excited

state character and consequently shows weak solvatochromism. At low excitation energy, 3.68 eV (337 nm), this emission is observed together with another peak around 450 nm. This second CT emission comes from molecules with the axial-equatorial conformation, $CT_{ax\text{-}eq}$, and shows strong solvatochromism. For higher energy excitation, 3.93 eV (316 nm), $CT_{ax\text{-}eq}$ is enhanced and becomes the dominant emission. **Figure 3** shows how the maximum intensity of each CT state in MCH solvent depends on the excitation energy. As can be seen, the emission which comes from the axial-axial conformation, $CT_{ax\text{-}ax}$, does not depend strongly on the excitation energy. However, the emission which comes from the axial-equatorial conformation, $CT_{ax\text{-}eq,}$ is enhanced when the excitation occurs in the absorption peak of the A and D units. When the molecules are excited at lower energy, i.e., at the edge of the absorption spectrum, both states emit equally and weakly. The emission spectra used to produce this data is shown in **Figure S6**.

Thus, higher excitation energy, with a high degree of excess energy, leads to the predominant formation of the $CT_{ax\text{-}eq}$ excited state, and we propose that the excess energy may enable molecular rearrangement from the ax-ax to the ax-eq conformation.

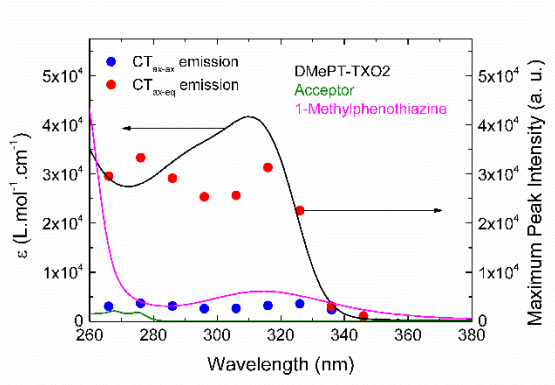


**Figure 3.** Maximum peak intensity of CT axial-axial emission (blue dot) and CT axial-equatorial emission (red dot) of DMePT-TXO2 in MCH solution at different energy excitations. Full lines are the same extinction coefficient data shown in Fig. 2a.

In toluene, the same behaviour is observed; the $CT_{eq}$ and $CT_{ex}$ emission have roughly the same relative contributions in the overall emission, but with a small red shift of the $CT_{ax}$ and a much larger red shift of the $CT_{eq}$. However, when the toluene solution is excited at higher energy, 3.93 eV (315 nm), the $CT_{eq}$ again dominates (**Figure S7**). Moving to even higher polarity, DCB solvent, the $CT_{eq}$ emission is dominant (337 nm excitation) and just a vestige of $CT_{ax}$ remains. This shows that the polarity of this environment is high enough to enable molecular rearrangement and hence strong stabilization of the $CT_{ax\text{-}eq}$ conformation, and high excitation energy is no longer needed. Thus, the contributions between the $CT_{eq}$ and $CT_{ax}$ emission can be controlled by increasing the excitation energy (excess energy), i.e., the $CT_{ax\text{-}eq}$ state has an energy barrier to formation/stabilization. However, in a high polarity environment (DCB solution) the ax-eq conformation is strongly stabilized even at low excitation energies so that predominantly $CT_{eq}$ emission is observed.

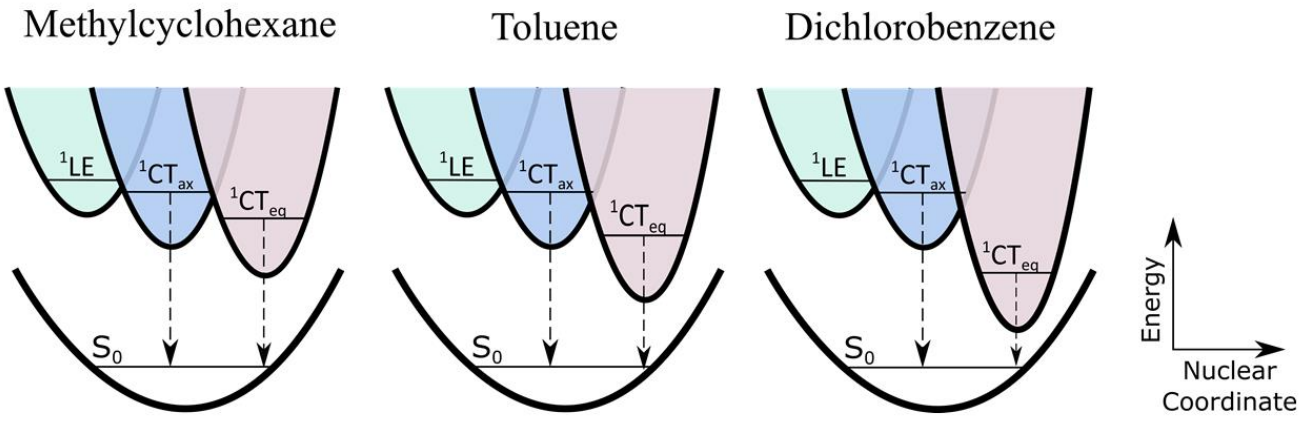


**Scheme 1.** Schematic energy level diagram of DMePT-TXO2 in different solvents. $^1LE$, $CT_{ax,}$ $CT_{eq}$ and $S_{0,}$ refers to: local excited state, axial charge transfer state, equatorial charge transfer state and ground state, respectively.

The peak emission of $CT_{ax}$ in MCH (337 nm excitation), toluene and DCB, are 371 nm, 391 nm and 407 nm, respectively. This leads to a red shift of 36 nm from the lowest-polarity to highest-polarity environment. The peak emission of $CT_{eq}$ in MCH, toluene and DCB, are 450 nm, 479 nm and 528 nm, respectively, showing a large red-shift of 78 nm (see **table S1**). These results enabled us to build a simple potential well scheme of the excited states ($^1$LE and $^1$CTs) in different solvent polarities (**Scheme 1**). As the solvent polarity increases, the CT energy levels start to decrease, because of the large dipole moment of the charge transfer states leading to strong screening of the Coulomb term by the reorganization of the solvent shell. On the other hand, $^1$LE remains nearly unchanged because its emission is not affected by the polarity of the solvent (**Figure S8**). In low-polarity solvents, the overall emission has strong LE character, and the energy difference between $CT_{eq}$ and $CT_{ax}$ is small. By increasing the solvent polarity, the CT states gradually red shift, resulting in less LE character and a higher energy difference between $CT_{ax}$ and $CT_{eq.}$ The contribution of triplet excited states to the overall emission was analyzed in DMePT-TXO2 (337 nm excitation) (**Figure S9**). The contributions are 10% for toluene and 16% for DCB.

**Figure 4a** shows the decay curves of DPT-TXO2 in different solvents. The curves are normalized for better comparison. The decay curves show two different regimes, a fast decay, associated to prompt CT emission (PF), and a slow decay, associated to the delayed fluorescence (DF). As expected, the DCB solution shows higher DF contribution because in this environment the DPT-TXO2 has the smallest CT-$^3$LE energy splitting ($\Delta E_{ST}$). **Figure 4b** shows the same analysis for DMePT-TXO2. The decay curves are in agreement with the degassing results, which show that the triplet contribution in DMePT-TXO2 is very low, with almost no DF emission. DMePT-TXO2 in MCH and toluene solvents show just prompt CT emission, no DF was observed.

However, in DCB the DF emission was identified, but is much weaker than that observed from DPT-TXO2.

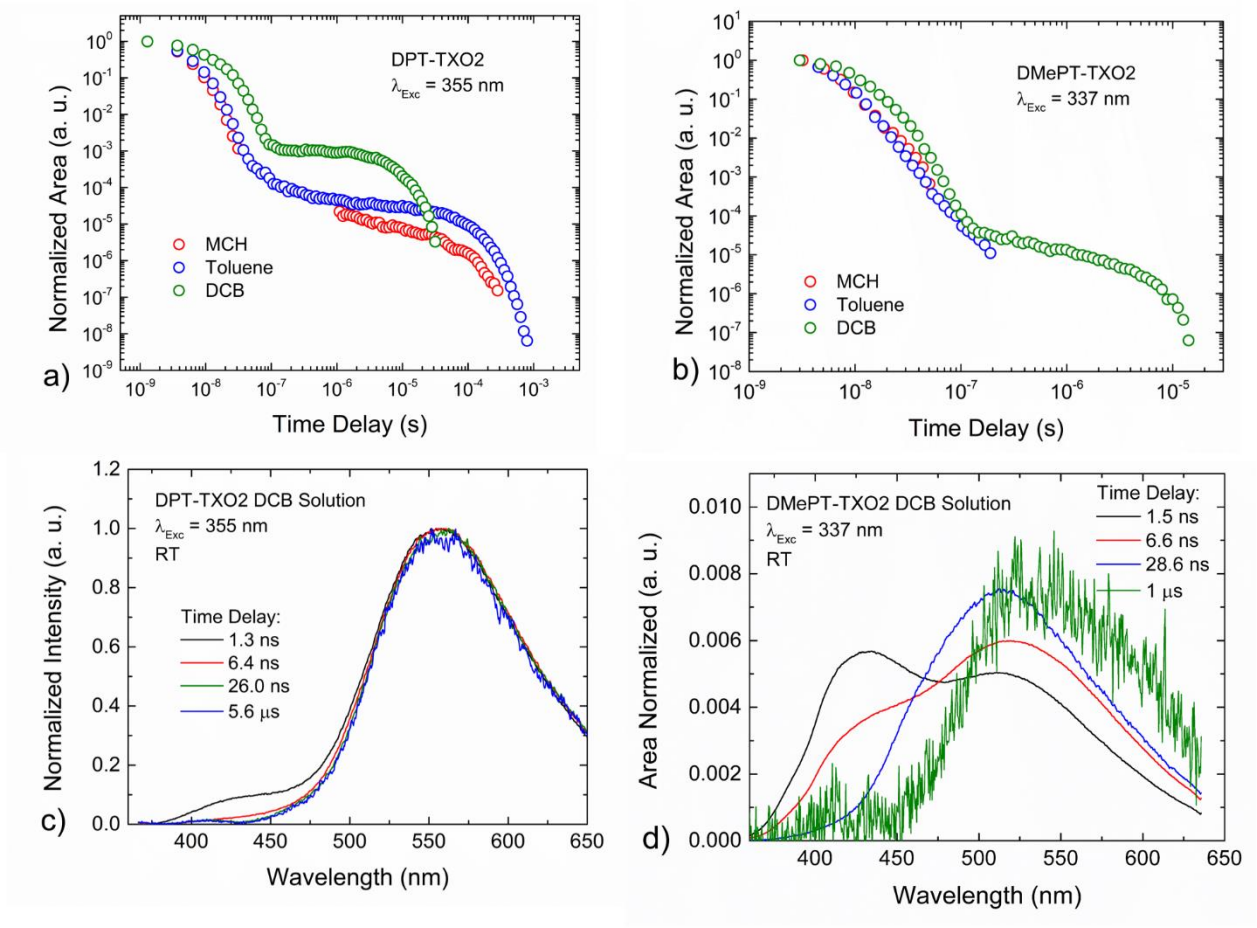


**Figure 4.** Time resolved fluorescence decay curves of a) DPT-TXO2 and b) DMePT-TXO2 molecules in different solvents: MCH, toluene and 1,2-dichlorobenzene (DCB). Time resolved normalized emission spectra in different time delays of collection of c) DPT-TXO2 and d) DMePT-TXO2 molecules in 1,2-dichlorobenzene (DCB) solvent. DPT-TXO2 molecules were excited at 355 nm and DMePT-TXO2 at 337 nm, all at RT.

DCB solutions show stabilized CT formation in both molecules, bringing CT closer to, and in resonance with, the $^3$LE state; thus we analyse the emission spectra in the PF and DF regions.

**Figure 4c** shows that DPT-TXO2 has almost the same emission spectra (shape and position) in the entire region of analyses, apart from a vestige of emission around 425 nm in earliest times which can be assigned to either donor emission or very weak $CT_{ax}$. The majority of the emission in both regions (PF and DF) comes from the same transition, $^1CT \rightarrow S_0$. The latest emission was collected at TD = 35 µs.

Analogous experiments were performed with DMePT-TXO2 (**Figure 4d**). In the first 10 nanoseconds, strong $CT_{ax}$ emission is observed competing with $CT_{eq}$ emission, and at later times, pure $CT_{eq}$ emission is detected. As both emissions are observed simultaneously and in these area normalized spectra an isoemissive point is observed, it is clear that they are independent states and that the $CT_{ax}$ states are not quenched by $CT_{eq}$. In the µs range, the emission was very weak, as can be seen at TD = 1 µs, and the last DF spectrum detected was at TD = 15 µs. The emission spectra of DMePT-TXO2 in DCB solution at different time delays were also analyzed for lower excitation energy, 355 nm (**Figure S10**). These results show that less $CT_{eq}$ states are formed compared to the case shown in **Figure 4d**; this is because in the first few nanoseconds the spectra show a higher contribution of $CT_{ax}$ than $CT_{eq}$.

Interestingly, in DCB, the $CT_{ax}$ state still lives a few nanoseconds, making it possible to detect clearly its emission in the iCCD camera. However, for MCH and toluene solutions, the $CT_{ax}$ emission is detected weakly, due to the very fast decay of this state in these less polar environments (See **Figure S10**). Thus, it suggests that the high polarity environment stabilizes the $CT_{ax,}$ even though its contribution, in the overall emission (PL spectra), is much weaker than the $CT_{eq}$ and the lifetime is much faster.

The intensity dependence of the DF emission in the DF region of both molecules was analyzed as a function of the laser excitation dose. A linear gradient of 0.970 ± 0.005 was found

for DPT-TXO2 and 1.19 ± 0.02 for DMePT-TXO2 (**Figure S11**). These results confirm the thermally assisted mechanism as opposed to triplet-triplet annihilation (TTA) for DPT-TXO2 and DMePT-TXO2 in DCB solvent.

Therefore, the analyses of the solution measurements show that the incorporation of a methyl group on the phenothiazine D units profoundly changes the photophysics of the D–A–D molecules. DMePT-TXO2 shows two clearly different CT states (337 nm excitation). These two CT states are correlated with two different conformations of the molecule. It is likely that when the molecules are excited at higher energies (high excess energy) or are in a high polarity environment, the initial configuration between D and A units, namely $CT_{ax\text{-}ax}$, can re-orient to yield the $CT_{ax\text{-}eq}$ configuration. However, at low excitation energies or low polarity environments, the formation of the weak CT state, $CT_{ax\text{-}ax,}$ is also strongly observed. Recent research has also enabled the observation of two switchable conformations for D–A–D molecules with phenothiazine donor units, due to the intrinsic nature of this donor unit, and its ability to form H-intra and H-extra folded conformers that allow formation of parallel quasi-axial and perpendicular quasi-equatorial CT states in the DPTZ-DBTO2 molecule.[11]

SOLID STATES PROPERTIES

The solid state properties of DPT-TXO2 and DMePT-TXO2 were analyzed in zeonex matrix (low polarity environment). **Figure S12** shows the steady steady emission of both molecules in air and under vaccum. DPT-TXO2 shows just $^1$CT emission in air and a large contribution of phosphorescence (PH) when the oxygen is removed. DMePT-TXO2 in zeonex shows results similar to that observed in MCH solution: two different CT states are observed; $CT_{ax\text{-}ax}$ around 370 nm, and $CT_{ax\text{-}eq}$ around 450 nm. When the oxygen is removed, a large contribution

of PH is also observed. Hence, three distinct emissions are observed simultaneously in DMePT-TXO2 zeonex film.

**Figure 5** shows how the maximum intensity of each CT state in zeonex matrix depends on the excitation energy. The emission spectra used to produce this data is shown in **Figure S13**. Contrary to the result in MCH, the maximum peak intensity of the CT states does not change much by changing the excitation energy. This can be attributed to the fact that in solid state, the molecules are confined and are not free to re-orient as in solution.

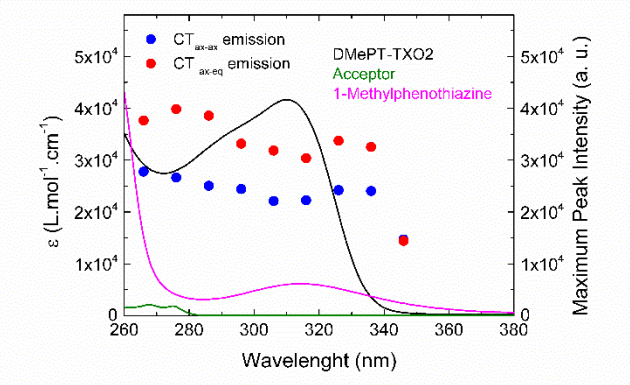


**Figure 5** Maximum peak intensity of CT axial-axial state (blue dot) and CT axial-equatorial state (red dot) of DMePT-TXO2 in zeonex matrix at different energy excitations. Full lines are the same extinction coefficient data shown in Fig. 2a.

**Figure 6a** shows the decay curve in different temperatures of DPT-TXO2 zeonex film. The PF emission does not show dependence with the temperature, however the DF emission shows higher intensity at higher temperatures, as expected for a TADF mechanism. **Figure 6c** shows the time resolved emission decay of DPT-TXO2 film at 80 K. In the first nanoseconds, DPT-TXO2 shows emission spectra that peaks around 450 nm. This emission is associated with the $^{1}$CT state; however, some emission from $^{1}$LE may occur because the $^{1}$CT is very close in energy to the donor unit emission. Increasing the time delay, the emission spectrum progressively shifts to longer wavelengths, moving from $^{1}LE_{D}$ to $^{1}$CT and then to $^{3}LE_{D}$.

The observed triplet emission comes from the localized triplet state of the donor unit, as seen by comparison of the PH spectra of DPT-TXO2 and pure phenothiazine taken with the same experimental conditions (**Figure S14**). DPT-TXO2 PH emission has a relatively long lifetime, and it was easily detected even after 89 ms. The same spectral analyses were made at 290 K (**Figure S15**). At higher temperature, the DF emission contribution, which comes from the $^{1}$CT states, is stronger, and the PH weaker, as expected for TADF, due to the increased thermally activated energy for rISC.

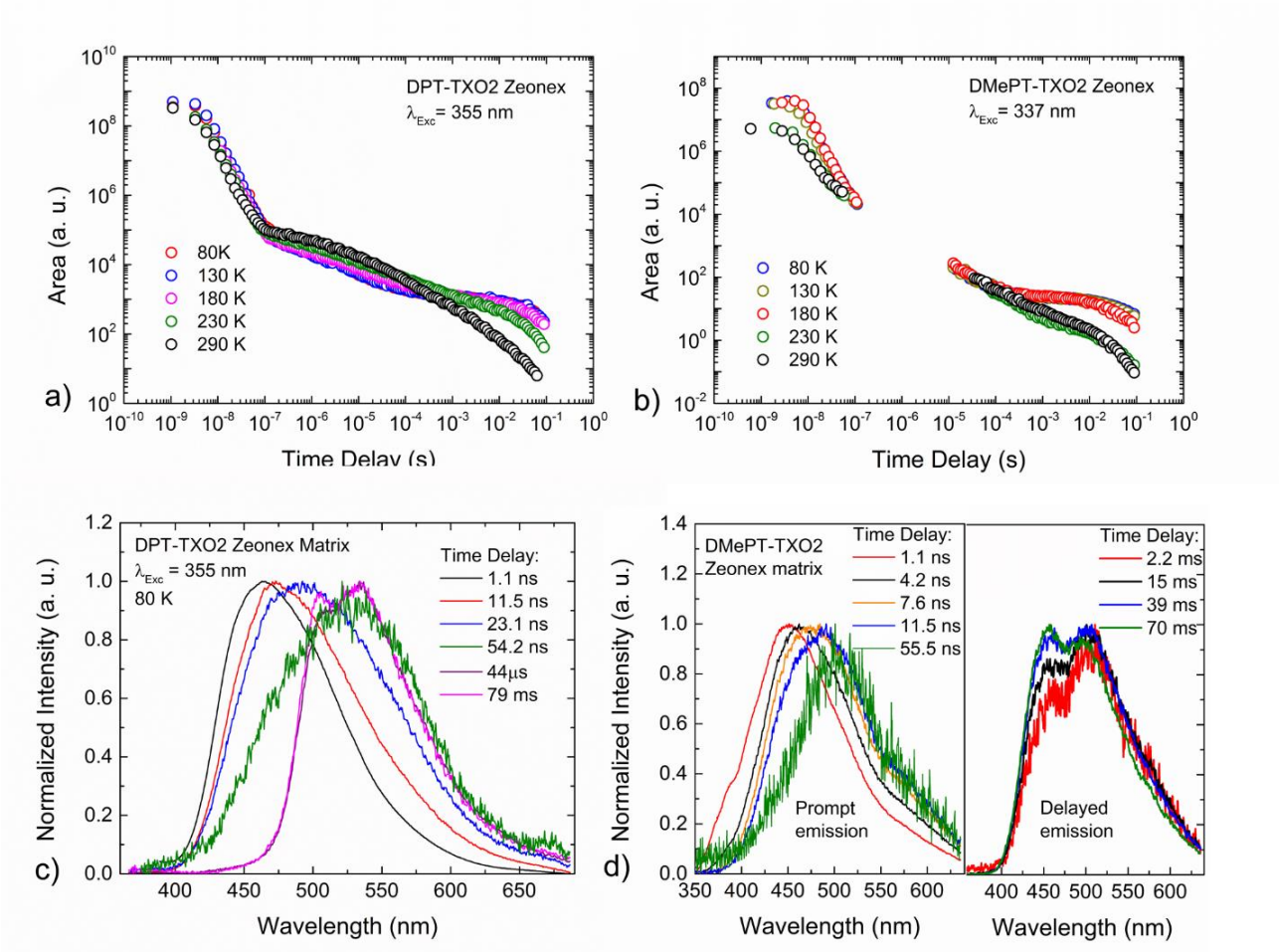


**Figure 6.** Time resolved fluorescence decay curves of a) DPT-TXO2 and b) DMePT-TXO2 in zeonex matrix at different temperatures. Time resolved normalized emission spectra in different

time delays of collection of c) DPT-TXO2 at 80 K and d) DMePT-TXO2 at 80 K. DPT-TXO2 molecules were excited at 355 nm and DMePT-TXO2 at 337 nm.

**Figure 6b** shows the decay curves for DMePT-TXO2 in zeonex matrix, excitation at 337 nm. Initially, a fast decay, related to the prompt emission, is observed, followed by an interval during which no emission was above the detection noise floor of the iCCD camera, and then, at longer time delays, phosphorescence appears. **Figure 6d** (left) shows the emission spectra in the PF region. At TD = 1.1 ns a shoulder around 375 nm is observed which may be associated with the $CT_{ax\text{-}ax}$ state, which has faster decay than $CT_{ax\text{-}eq}$. As the TD increases, the $CT_{eq}$ emission shows a slight red shift to ca. 400 nm, and can be associated with the relaxation of this state, as also seen in the DPT-TXO2. The emission spectra in the PH region, **Figure 6d** (right), shows an interesting feature. As the TD increases, an emission on the blue edge of the spectra grows in. This PH emission on the blue edge is assigned as the PH from the axial conformation, $^3LE_{ax}$, which acts as an effective loss pathway in the emission of this molecule. This higher energy triplet state cannot couple with the $^1CT_{eq}$ state identified in the prompt emission, thus the rISC is suppressed and any TADF is observed.

The photoluminescence quantum yields (PLQY) of each material also show strong dependence on the TADF mechanism. DPT-TXO2 in zeonex matrix has PLQY values of (10±1)%, in nitrogen atmosphere and (4.2±0.4)% in air. Whereas, DMePT-TXO2 has PLQY values of (4.5±0.4)% in nitrogen atmosphere and (4.1±0.4)% in air. The latter values are very close each other, due the fact that DMePT-TXO2 has no TADF contribution in zeonex matrix, therefore the PLQY value is not enhanced by removing the oxygen (See **table S2**).

**Figure 7a and b** show the PH time dependent spectra with different excitation energies, and longer integration time than the spectra showed in **Figure 6d**. The PH spectra of the donor and acceptor units in pristine film are also displayed, in dash-lines, for comparison. The PH spectrum of 1-methylphenothiazine is very similar to phenothiazine, and we have previously reported the PH spectrum of the acceptor unit.[21]

With excitation at 355 nm, the earliest PH spectrum displayed in the graph (TD = 2 ms) shows just a shoulder due to the $^3LE_{ax}$ contribution, as described above. For excitation at 266 nm, the PH shows a different feature. A PH emission from the A units is also observed, which becomes the dominant triplet emission at later TD. This strong triplet emission arises from the strong absorption of the A units at 266 nm (See **Figure 2a**). Both $^3LE_A$ and $^3LE_{D,}$ emit strongly until the end of the measurement (TD=89 ms).

Therefore, the PH of DMePT-TXO2T in zeonex matrix highlights different features at different excitations energies. Excitation at higher energy shows dual PH emission from the $^3LE$ states of both the donor and acceptor units, which behave as independent emitting species, showing that the D and A units of these molecules are totally electronically decoupled. The contribution from the acceptor is stronger at later times, indicating a longer triplet state lifetime. On the other hand, for DPT-TXO2 in zeonex matrix, the PH spectra come from the lowest triplet state, $^3LE_D$ which may imply some D–A conjugation within the molecules.

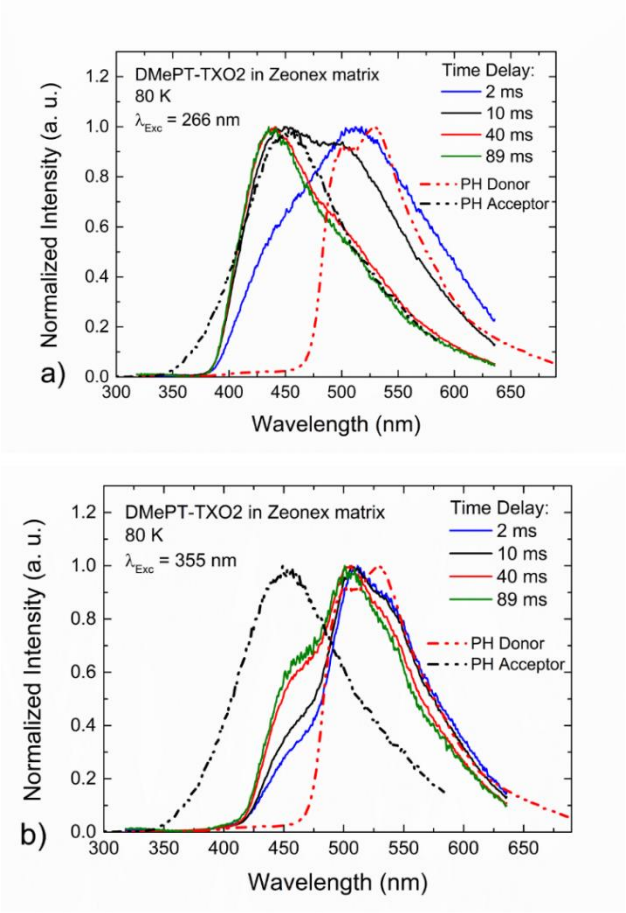


**Figure 7.** a) Time resolved normalized emission spectra of DMePT-TXO2 in the phosphorescence emission region for excitation at a) 266 nm and b) 355 nm at 80 K.

Regarding the $^1$CT-$^3$LE energy splitting, $\Delta E_{ST}$, DMePT-TXO2 should show more efficient TADF than DPT-TXO2. Both molecules have similar $^1CT_{eq}$ states, but DMePT-TXO2 has closer local triplet levels, due to the contribution of the $^3LE_{ax}$. However, $^3LE_{ax}$ cannot couple with $^1CT_{eq}$, and the $^1CT_{ax}$ has much higher energy, resulting in a huge energy gap between $^1CT_{ax}$ and $^3LE_{ax}$, suppressing any rISC process.

Therefore, the solid-state analysis reveals that the methyl group incorporated in the D units also gives rise to the formation of two distinct PH states, $^3LE_{eq}$ and $^3LE_{ax;}$ the latter one does not

undergo rISC, preventing the TADF mechanism from occurring and giving rise to PH at RT. The $^3LE_{ax}$ state thus is an energy sink in the DMePT-TXO2 system, as has also been observed in other molecules where phenothiazine is in an axial conformation.[11]

## CONCLUSION

In summary, DMePT-TXO2 molecules shows dual fluorescence clearly coming from two different CT states in solution and solid state. These two CT states are correlated with two different conformations of the molecule. Likely, when the molecules are excited at higher energies (high excess energy) or are in a high polarity environment (polar solvents), the initial configuration between D and A units $CT_{ax\text{-}ax}$ can re-orient to yield the $CT_{ax\text{-}eq}$ configuration. However, when molecular motion is suppressed, by dispersing the molecules in a solid state host, this re-orientation is not observed and strong phosphorescence at room temperature is detected, besides the fluorescence emission.

Additionally, the solid state analysis enables an in-depth study of the triplet states of these D–A–D molecules. Experiments identify that the PH of DMePT-TXO2 has a main contribution from $^3LE_{eq}$ but also shows $^3LE_{ax}$ emission. Regarding the TADF mechanism, DPT-TXO2 molecules show repopulation of the $^1CT$ state *via* a reverse intersystem crossing process in solutions and solid state. On the other hand, DMePT-TXO2 molecules show this characteristic only in polar solutions, that is in an environment where the molecules are free to rotate; in contrast, in the solid state, the rISC process is completely suppressed.

Therefore, the comparison between DPT-TXO2 and DMePT-TXO2 is important for gaining a better understanding about the subtle relationship between molecular conformation of

the constituent units and the TADF mechanism, making easier the design of novel TADF materials in the future.

ASSOCIATED CONTENT

Supporting Information available: Synthetic details, additional X-ray data and additional photophysical data.

**Corresponding Author**

*Prof. Andrew P. Monkman (a.p.monkman@durham.ac.uk)

**Author Contributions**

P. L. dos Santos performed photophysical experiments and analyzed the data. J. S. Ward and M. R. Bryce designed and synthesized both molecules. Andrei S. Batsanov performed and analyzed the X-ray study. P. L. dos Santos and A. P. Monkman determined the phenomenology of the results and wrote the manuscript with contributions from all authors. All authors gave approval to the final version of the manuscript.

ACKNOWLEDGMENT

P. L. dos Santos thanks CAPES Foundation, Ministry of Education of Brazil, Brasilia - DF 70040 - 020, Brazil, in particular the Science Without Borders Program for a PhD studentship, Proc. 12027/13-8. J. S. Ward thanks EPSRC for funding. All authors thank EPSRC grant EP/L02621X/1. We also thank Hamamatsu for providing the PLQY equipment (Quantaurus – QY).

REFERENCES


(1) Tang, C. W.; VanSlyke, S. A. Organic Electroluminescent Diodes. *Appl. Phys. Lett.* **1987**, *51* (12), 913–915.

(2) Dias, F. B. Kinetics of Thermal-Assisted Delayed Fluorescence in Blue Organic Emitters with Large Singlet – Triplet Energy Gap *Proc. Roy. Soc* **2015**, *373*, 20140447.

(3) Dias, F. B.; Bourdakos, K. N.; Jankus, V.; Moss, K. C.; Kamtekar, K. T.; Bhalla, V.; Santos, J.; Bryce, M. R.; Monkman, A. P. Triplet Harvesting with 100% Efficiency by Way of Thermally Activated Delayed Fluorescence in Charge Transfer OLED Emitters. *Adv. Mater.* **2013**, *25* (27), 3707–3714.

(4) Goushi, K.; Yoshida, K.; Sato, K.; Adachi, C. Organic Light-Emitting Diodes Employing Efficient Reverse Intersystem Crossing for Triplet-to-Singlet State Conversion. *Nat. Photonics* **2012**, *6* (4), 253–258.

(5) Numata, M.; Yasuda, T.; Adachi, C. High Efficiency Pure Blue Thermally Activated Delayed Fluorescence Molecules Having 10H-Phenoxaborin and Acridan Units. *Chem. Commun.* **2015**, *51*, 9443–9446.

(6) dos Santos, P. L.; Ward, J. S.; Bryce, M. R.; Monkman, A. P. Using Guest–Host Interactions to Optimize the Efficiency of TADF OLEDs. *J. Phys. Chem. Lett.* **2016**, 3341–3346.

(7) Gibson, J.; Monkman, A.; Penfold, T. The Importance of Vibronic Coupling for Efficient Reverse Intersystem Crossing. *ChemPhysChem* **2016**, *17*, 2956–2961.

(8) Etherington, M. K.; Gibson, J.; Higginbotham, H. F.; Penfold, T. J.; Monkman, A. P.; Revealing the Spin–vibronic Coupling Mechanism of Thermally Activated Delayed Fluorescence. *Nat. Commun.* **2016**, *7*, 13680.

(9) Ward, J. S.; Nobuyasu, R. S.; Batsanov, A. S.; Data, P.; Monkman, A. P.; Dias, F. B.; Bryce,

M. R. The Interplay of Thermally Activated Delayed Fluorescence (TADF) and Room Temperature Organic Phosphorescence in Sterically-Constrained Donor–acceptor Charge-Transfer Molecules. *Chem. Commun.* **2016**, *52*, 2612-2615.

(10) Okazaki, M.; Takeda, Y.; Data, P.; Pander, P.; Higginbotham, H.; Monkman, A. P.; Minakata, S. Thermally Activated Delayed Fluorescent Phenothiazine-Dibenzo[a,j]phenazine-Phenothiazine Triads Exhibiting Tricolor-Changing Mechanochromic Luminescence. *Chem. Sci.* **2017**, 1–10.

(11) Etherington, M. K.; Franchello, F.; Gibson, J.; Northey, T.; Santos, J.; Ward, J. S.; Data, P.; Kurowska, A.; dos Santos, P. L.; Graves, D. R. et al. Regio- and Conformational Isomerisation Critical to Design of Efficient Thermally-Activated Delayed Fluorescence Emitters. *Nat. Commun.* **2017**, *8*, 14987.

(12) Tanaka, H.; Shizu, K.; Nakanotani, H.; Adachi, C. Dual Intramolecular Charge-Transfer Fluorescence Derived from a Phenothiazine-Triphenyltriazine Derivative. *J. Phys. Chem. C* **2014**, *118* (29), 15985–15994.

(13) Sheldrick, G. M. A Short History of SHELX. *Acta Crystallogr. Sect. A Found. Crystallogr.* **2008**, *64* (1), 112–122.

(14) Sheldrick, G. M. SHELXT - Integrated Space-Group and Crystal-Structure Determination. *Acta Crystallogr. Sect. A Found. Crystallogr.* **2015**, *71* (1), 3–8.

(15) Dolomanov, O. V.; Bourhis, L. J.; Gildea, R. J.; Howard, J. A. K.; Puschmann, H. OLEX2: A Complete Structure Solution, Refinement and Analysis Program. *J. Appl. Crystallogr.* **2009**, *42* (2), 339–341.

(16) Spek, A. L. PLATON SQUEEZE: A Tool for the Calculation of the Disordered Solvent Contribution to the Calculated Structure Factors. *Acta Crystallogr. D* **1990**, *71* (46), 194–

201.

(17) Chu, S. S. C.; Chung, B. J ; *Acta Cryst.* **1974**, *571*, 1616–1618.

(18) Stockmann, A.; Kurzawa, J.; Fritz, N.; Acar, N.; Schneider, S.; Daub, J.; Engl, R.; Clark, T. Conformational Control of Photoinduced Charge Separation within Phenothiazine-Pyrene Dyads. *J. Phys. Chem. A* **2002**, *106* (34), 7958–7970.

(19) Marian, C. M. Spin-Orbit Coupling and Intersystem Crossing in Molecules. *Wiley Interdiscip. Rev. Comput. Mol. Sci.* **2012**, *2* (2), 187–203.

(20) Penfold, T. J. On Predicting the Excited-State Properties of Thermally Activated Delayed Fluorescence Emitters. *J. Phys. Chem. C* **2015**, *119* (24), 13535–13544.

(21) Santos, P. L.; Ward, J. S.; Data, P.; Batsanov, A. S.; Bryce, M. R.; Dias, F. B.; Monkman, A. P. Engineering the Singlet–triplet Energy Splitting in a TADF Molecule. *J. Mater. Chem. C* **2016**, *4*, 3815-3824.

(22) Youn Lee, S.; Yasuda, T.; Nomura, H.; Adachi, C. High-Efficiency Organic Light-Emitting Diodes Utilizing Thermally Activated Delayed Fluorescence from Triazine-Based Donor-Acceptor Hybrid Molecules. *Appl. Phys. Lett.* **2012**, *101* (9), 1–5.

(23) Dias, F. B.; Santos, J.; Graves, D.; Data, P.; Nobuyasu, R. S.; Fox, M. A.; Batsanov, A. S.; Palmeira, T.; Berberan-Santos, M. N.; Bryce, M. R.; Monkman, A. P. The Role of Local Triplet Excited States in Thermally-Activated Delayed Fluorescence: Photophysics and Devices. *Adv. Sci.* **2016**, *3*, 1600080.

**TOC GRAPHICS**